

Modelling of JT-60U Detached Divertor Plasma using SONIC code

Kazuo HOSHINO, Katsuhiko SHIMIZU, Tomonori TAKIZUKA,
Nobuyuki ASAKURA and Tomohide NAKANO

Japan Atomic Energy Agency, Naka, Ibaraki 311-0193, Japan

(Received: 20 November 2009 / Accepted: 22 March 2010)

The characteristics of the JT-60U detached divertor plasma in the SONIC simulation are investigated. With increasing mid-plane density, the electron temperature at the divertor decreases and the ion flux to the divertor plate increases. At higher densities, the temperature becomes less than 1 eV. However, rollover of the ion flux at the divertor plate, which is a characteristic of the detachment, is not observed. In order to improve the modelling of the detachment, the effects of some assumptions in the model on the divertor plasma characteristics are investigated. In the case with the wall pumping effect and low chemical sputtering, rollover of the ion flux appears. The low recycling and low sputtering yield prevent radiation cooling near the X-point. The appearance of rollover is possibly explained by the decrease in the ionization and the increase in the volume recombination associated with the high upstream density without the large radiation cooling near the X-point.

Keywords: SOL/Divertor code, integrated modelling, divertor plasma detachment, wall pumping, chemical sputtering, supersonic flow

1. Introduction

The large heat load to the divertor plate is one of the critical issues for magnetic fusion devices. The detached divertor operation is the most promising candidate to reduce the heat load to less than the engineering requirement ($\sim 10 \text{ MW/m}^2$). Detached divertor plasmas have been observed in many devices. With increasing upstream (core) density, the electron temperature at the target plate decreases and the ion flux initially increases. With higher upstream density, the electron temperature becomes less than 5 eV. The ion flux rolls over and then significantly decreases. Rollover of the ion flux to the target is one of important features of the divertor plasma detachment.

Charge-exchange by recycled neutrals and radiation cooling by impurities have important roles in removal of the parallel momentum and the energy, respectively. To reduce the ion flux toward the divertor plate, volume recombination and radial transport are essential. However, present understanding of the detachment is not enough to quantitatively explain the detachment observed in experiments.

A number of divertor codes are being developed to analyze and predict the SOL/divertor plasma characteristics, such as the heat and particle loads to the divertor, the SOL flow pattern, and the neutral and impurity transport. However, it seems to be challenging even for major two dimensional divertor codes to reproduce the detached divertor plasma observed in the

experiments [1]. The effort to improve the modelling of the divertor detachment is in progress under the International Tokamak Physics Activity (ITPA) SOL and Divertor Topical Group [2].

In this paper, modelling of the JT-60U detached divertor plasma is attempted using a suite of integrated codes SONIC [3, 4]. To improve the detachment modelling, the dependency of the divertor plasma characteristics on some assumptions, such as chemical sputtering, wall recycling, and boundary conditions, are also investigated.

2. Numerical model

A suite of integrated codes SONIC [3, 4] is applied to the analysis of the JT-60U detached divertor plasma. The SONIC suite consists of the 2D plasma fluid code (SOLDOR), the neutral Monte-Carlo code (NEUT2D) and the impurity Monte-Carlo code (IMPIC).

The transport of bulk ion D^+ is described in the fluid approximation by the SOLDOR code. The particle balance, parallel momentum balance, and ion and electron energy balance equations are solved. The perpendicular transport is assumed to be anomalous. The anomalous transport coefficients for the particle and heat transport are taken to be $D = 0.3 \text{ m}^2/\text{s}$ and $\chi_i = \chi_e = 1.0 \text{ m}^2/\text{s}$, respectively. On the other hand, the parallel transport along field lines in the SOL region is assumed to be classical. In the present version of SOLDOR, the effects of drifts and current are neglected.

author's e-mail: hoshino.kazuo@jaea.go.jp

Table 1 Atomic and molecular processes taken into account by SONIC. (I-e: electron impact ionization, CX: charge exchange, EL: elastic collision, DS: dissociation, RC: recombination)

Atom		
I-e	$e + D \rightarrow e + D^+ + e$	
CX	$D^+ + D \rightarrow D + D^+$	
EL	$D^+ + D \rightarrow D^+ + D$	
Molecule		
I-e	$e + D_2 \rightarrow e + D_2^+ + e$	
DS	$e + D_2 \rightarrow e + D + D$	
DS	$e + D_2 \rightarrow e + D^+ + D + e$	
EL	$D^+ + D_2 \rightarrow D^+ + D_2$	
Ion		
DS	$e + D_2^+ \rightarrow e + D^+ + D$	
DS	$e + D_2^+ \rightarrow e + D^+ + D^+ + e$	
DS	$e + D_2^+ \rightarrow D + D$	
RC	$e + D^+ \rightarrow D$	

The transport of neutral atom D and molecule D_2 are traced by the neutral Monte-Carlo code NEUT2D. As shown in table 1, the important atomic and molecular processes for appropriate treatment of the recycling are taken into account.

The Monte-Carlo code IMPMC is used for transport of carbon impurity species C^0 - C^{6+} , while most of other divertor codes treat the impurity species as fluid species. The Monte-Carlo model is suitable for taking into account the important processes for the impurity transport, such as interactions with walls/divertor, kinetic effects, dissociation processes of hydrocarbon and so on. On the other hand, disadvantages of the Monte-Carlo approach are large Monte-Carlo noise, large computer resource etc. Recently, these disadvantages have been overcome, and the IMPMC code has been self-consistently integrated with SOLDOR/NEUT2D [4]. In the present study, the complex dissociation processes of hydrocarbon are simplified to the ionization process of C atoms with a low energy (~ 1 eV), as in other divertor codes.

Figure 1 shows the numerical grid generated from the JT-60U MHD equilibrium of shot #39090. The basic parameters of this shot are as follows: the plasma current is $I_p = 1.6$ MA, the toroidal magnetic field is $B_T = 3.1$ T, the effective safety factor is $q_{eff} = 4.8$, and the NBI heating power is $P_{NBI} = 4.5$ MW. To deal with the complex divertor geometry and short mean-free path of neutral particles in high recycling divertor plasma, fine grids are adopted in the divertor region.

The plasma boundary at the core interface is set at $r/a = 0.95$. The total input power across the core interface boundary is set to $Q_{in} = 3.2$ MW. The particle flux across the core boundary Γ_{ion} and D_2 gas puff rate Γ_{puff} are varied within the range $1.0 \times 10^{21} \text{ s}^{-1} \leq \Gamma_{ion} \leq 3.0 \times 10^{21} \text{ s}^{-1}$ and $0 \text{ s}^{-1} \leq \Gamma_{puff} \leq 2.7 \times 10^{21} \text{ s}^{-1}$, respectively, to investigate the

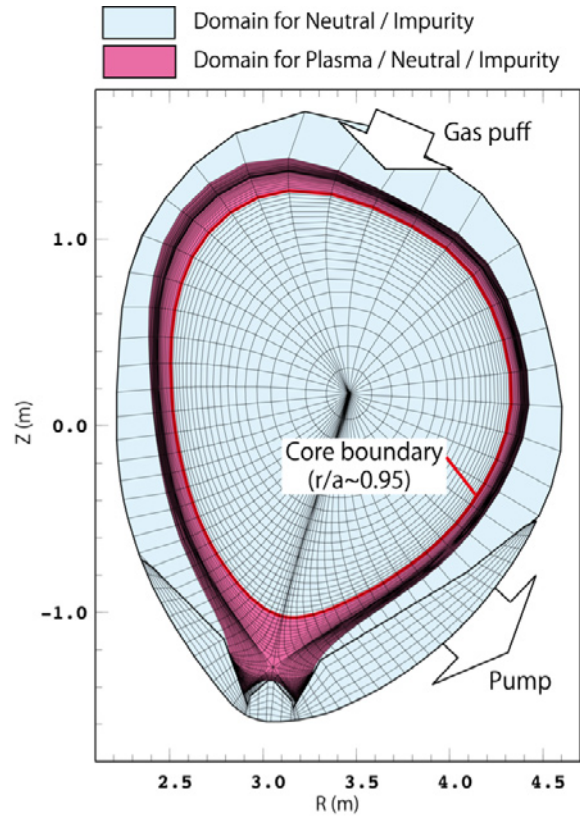


Fig. 1 Numerical grid for the SONIC simulation. Plasma is solved on the fine grid, while neutral and impurity particles are traced in the whole region. D_2 gas puff port locates at the upside.

divertor plasma characteristics. At the divertor plate, the usual Bohm condition is assumed.

The recycling coefficient R at the divertor and the wall is set to 1.0. At the pumping port shown in Fig. 1, the albedo for neutral particles is chosen to satisfy an effective pumping speed of $S_{pump} = 26 \text{ m}^3/\text{s}$. The chemical sputtering yield is assumed to be $Y_{ch} = 2\%$ on all plasma facing materials.

3. Simulation results

Figure 2 shows the 2D spatial profiles of the ion density n_i and the electron temperature T_e for the low density case ($n_{mid} = 0.5 \times 10^{19} \text{ m}^{-3}$) and the high density case ($n_{mid} = 1.3 \times 10^{19} \text{ m}^{-3}$), where n_{mid} is the ion density at the outer mid-plane separatrix (OMP). In the low n_{mid} case (Figs. (a) and (c)), the high temperature plasma ($T_e > 10$ eV) reaches the divertor and the ion density is low. At the outer strike point (OSP), $T_e = 30$ eV and $n_i = 1.6 \times 10^{19} \text{ m}^{-3}$. The outer divertor region is in the low-recycling regime. On the other hand, in the high n_{mid} case (Figs. (b) and (d)), the high temperature region is clearly separated from the target plate. A low T_e region (< 3 eV) is along the separatrix and reaches to the X-point. The ion density is high in the whole divertor region compared

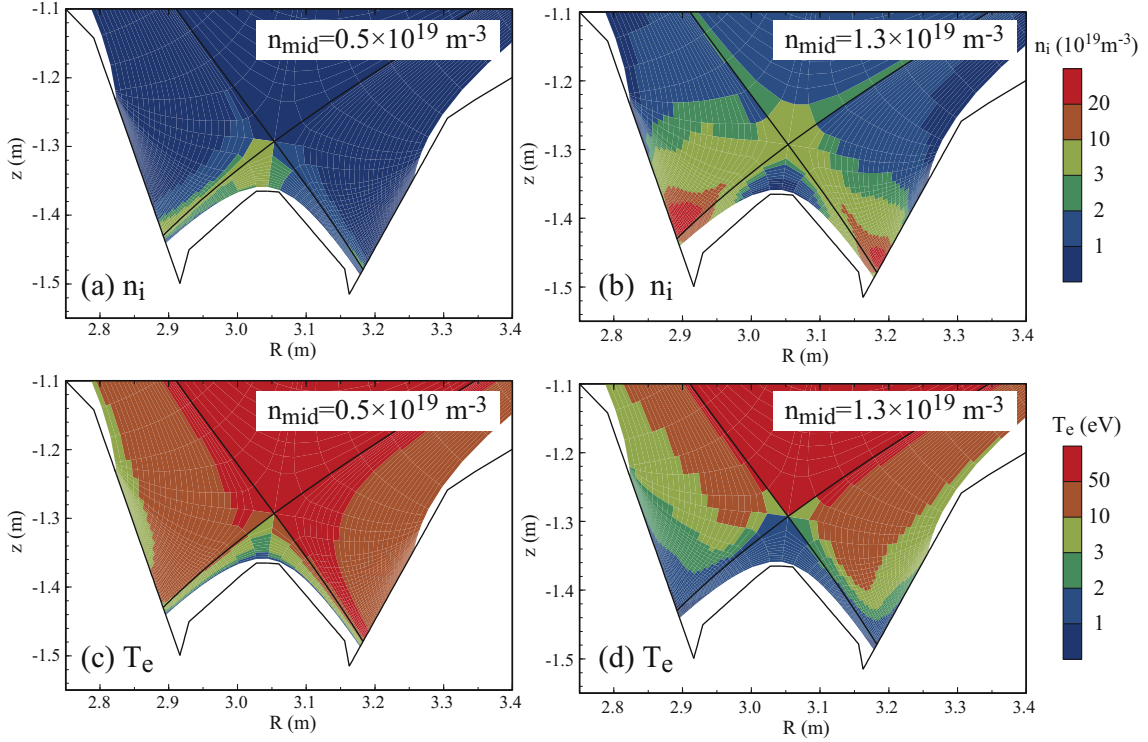


Fig. 2 2D spatial profile of the ion density (a) and (b), and the electron temperature (c) and (d). The low mid-plane density ($n_{mid} = 0.5 \times 10^{19} \text{ m}^{-3}$) case is shown in (a) and (c), while (b) and (d) show the high density case ($n_{mid} = 1.3 \times 10^{19} \text{ m}^{-3}$).

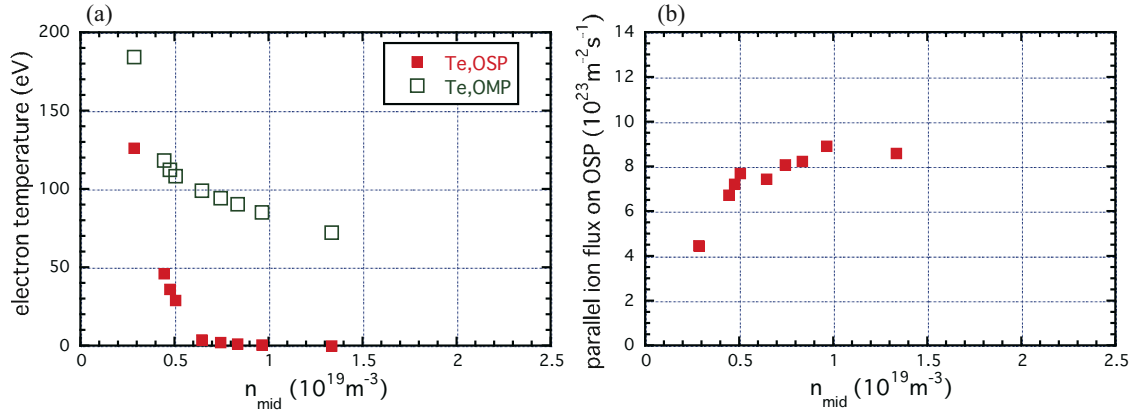


Fig. 3 The electron temperature and the parallel ion flux are plotted as a function of n_{mid} . The close and open symbols indicate the outer strike point (OSP) and the outer mid-plane (OMP), respectively.

with the low n_{mid} case.

In Fig. 3, the electron temperature and the ion flux at the outer strike point are plotted as a function of n_{mid} . With increasing n_{mid} , the electron temperature at the OSP significantly decreases compared with that at the OMP, and the ion flux increases. In the range $n_{mid} > 0.6 \times 10^{19} \text{ m}^{-3}$, T_e becomes less than a few eV. However, the ion flux does not decrease. The rollover of the ion flux, which is a feature of the detachment, cannot be reproduced. The ion flux possibly decreases at the higher density. However, if n_{mid} increases further, a large amount of impurity radiation near the X-point disrupts the edge plasma. Therefore, the

simulation is abnormally terminated.

4. Effect of assumptions on the detachment

In the above simulation, the characteristic of the detachment, i.e., rollover and significant reduction of the ion flux associated with increase in n_{mid} , cannot be seen. In order to clarify the key mechanism of reduction of the ion flux, effects of the following assumptions on the divertor plasma characteristics are investigated: Sec. 4.1 chemical sputtering yield, Sec. 4.2 recycling coefficient for neutral particles and Sec. 4.3 boundary condition at

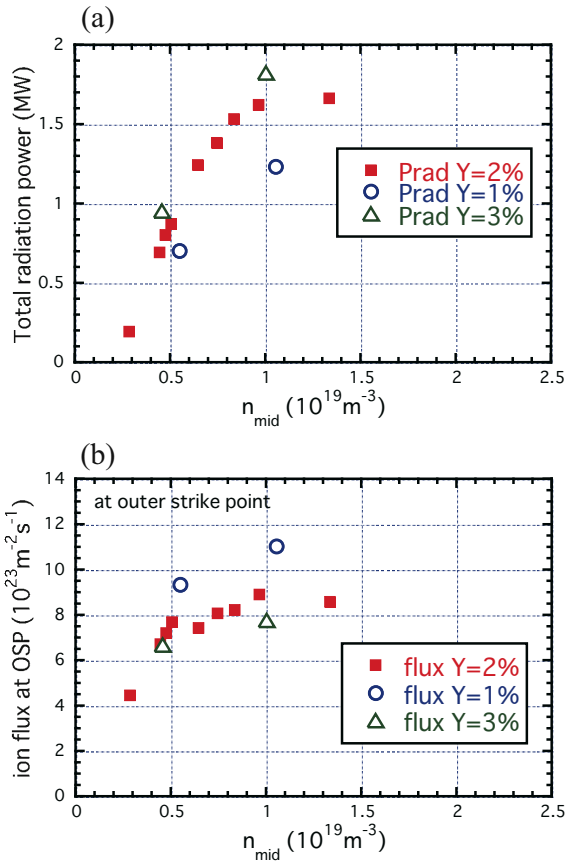


Fig. 4 The effect of the chemical sputtering yield: (a) total radiation power P_{rad} and (b) ion flux. The square symbol is the reference case, which is shown in Sec. 3. The circle and triangle symbols are the $Y_{ch}=1\%$ and $Y_{ch}=3\%$ case, respectively.

the target plate.

4.1. Effect of chemical sputtering yield

In the numerical analysis using a divertor code, the chemical sputtering yield Y_{ch} is often assumed to be $Y_{ch} = 1 \sim 5\%$. To investigate the effect of Y_{ch} on the divertor plasma characteristics, the cases with $Y_{ch} = 1\%$ and $Y_{ch} = 3\%$ are performed in addition to the $Y_{ch} = 2\%$ case, which was shown in Sec. 3. In Fig. 4, the total radiation power and the ion flux at OSP for $Y_{ch} = 1\%$ and $Y_{ch} = 3\%$ cases are plotted as a function of n_{mid} . As a reference case, the $Y_{ch} = 2\%$ case is also shown by the square symbols. With increasing chemical sputtering yield, the total radiation power increases, as shown in Fig. 4(a). Therefore, the electron temperature becomes low. The ionization decreases and the volume recombination increases. As a result, the ion flux decreases. However, the effect of the chemical sputtering yield on the n_{mid} dependency seems to be small. A significant reduction of the ion flux is not seen even in the $Y_{ch} = 3\%$ case. As in the reference case, the SONIC simulation of the higher density case is terminated by a large amount of impurity

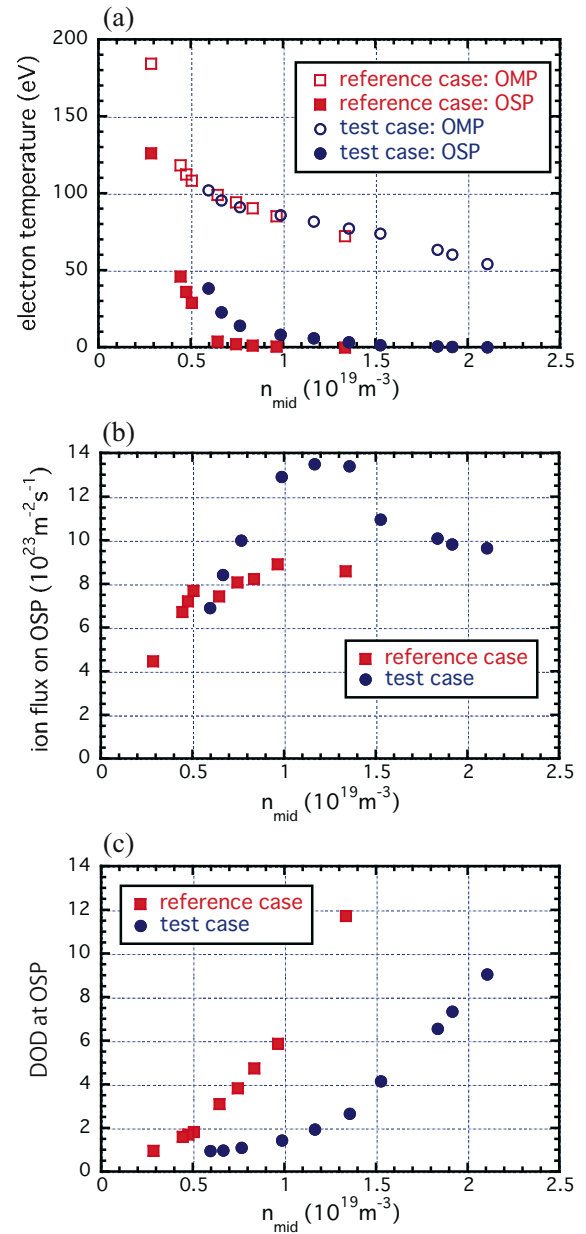


Fig. 5 The effect of the wall pumping with the low chemical sputtering yield: (a) electron temperature, (b) ion flux, and (c) degree of detachment (DOD) [5] at the OSP. The circle and square symbols correspond to the test case and the reference case ($R = 1$ and $Y_{ch} = 2\%$ case), respectively.

radiation near the X-point.

4.2. Effect of wall recycling

In the simulation, a saturated wall, i.e., $R = 1$, is often assumed. However, in the experiments, the wall is not always saturated. In addition, hydrocarbons that are chemically sputtered from the wall deposit onto the shadow area. These effects act as an effective particle sink in the system. Such effects are investigated by changing the recycling coefficients. In the test case, the recycling coefficients are set to $R_{wl} = 0.99$ and $R_{va} = 0.98$, where R_{wl}

and R_{va} are the recycling coefficient at the wall/divertor and vacuum region, respectively. In addition, the chemical sputtering yield is set to 1%.

Figure 5 shows the effect of low R and low Y_{ch} . In the test case, $T_{e,OSP}$ is higher than that in the reference case due to the small amount of the recycling and the impurity radiation. As shown in Fig. 5(b), rollover of Γ_{OSP} can be clearly seen in the test case. However, the reduction of the ion flux after the rollover is small compared with the experiment.

The degree of detachment (DOD) [5] is shown in Fig. 5(c). (DOD is defined by $DOD = \Gamma_{cal}/\Gamma_d$, where Γ_d is the ion flux to the target plate and $\Gamma_{cal} \propto n_{mid}^2$ is the ion flux calculated by the simple two-point model). The DOD in the reference case begins to rise at low mid-plane density. The weak detachment starts in the reference case. However a large amount of the impurity radiation near the X-point disrupt the edge plasma before the rollover. In the test case, the low recycling and the low sputtering yield prevent significant radiation cooling near the X-point. In the divertor region, the volume recombination increases because T_e decreases with increasing n_{mid} . Therefore, the test case can reach the rollover of the ion flux before the disruption by the large radiation cooling.

4.3. Effect of supersonic flow

In the plasma fluid model, $M=1$ is often assumed at the sheath entrance, where M is the Mach number. However, the Bohm criterion gives only the lower limit of the Mach number, i.e., $M \geq 1$, at the sheath entrance. The solution of the supersonic flow ($M > 1$) at the sheath entrance was shown analytically and numerically in Ref. [6-9]. In the weak detachment phase, T_e near the divertor plate is less than a few eV mainly due to the impurity radiation. As a result, the ionization region separates from the momentum loss region, which is just in front of the target plate. In the ionization region, the pressure gradient becomes steep because T_e significantly decreases along the field line toward the divertor plate. The steep pressure gradient without the momentum loss drives the high Mach flow near the X-point [7]. If the momentum loss near the target plate is small, the parallel ion flow is further accelerated toward the target plate, i.e., the supersonic flow (SSF) is driven. In ref. [8], the SSF was investigated using a particle simulation code, and the possibility of a reduction of the parallel ion flux by SSF was pointed out.

The effect of the SSF on the ion flux reduction is investigated by changing the boundary condition at the target. The highest n_{mid} case in section 4.2, i.e., the wall pumping case, is chosen as a reference case. The Mach number at the sheath entrance is set to $M=3$ and 10 at $0 \text{ cm} < d_{sep} < 5.8 \text{ cm}$, where d_{sep} is the radial distance from the separatrix. The radial profiles of the ion density and the ion flux at the outer target are shown in Fig. 6. The ion density

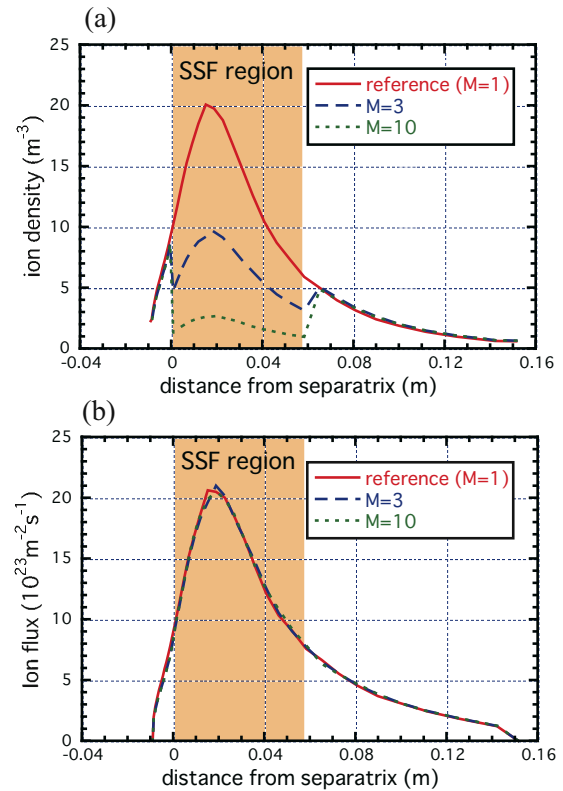


Fig. 6 Radial profile at the outer target: (a) ion density and (b) ion flux. Solid line is the reference case ($M=1$). Broken and dotted lines are the $M=3$ case and $M=10$ case, respectively.

at the target decreases in the SSF region. However the ion flux does not change. In the condition of the reference case, most of the ion flux to the divertor target is the ion flux from upstream rather than the particle source just in front of the divertor. Therefore, the effect of the SSF on the Γ_d is small, although the ion density at the target is significantly decreased by the SSF.

5. Summary

The characteristics of the JT-60U detached divertor plasma in the SONIC simulation were investigated. As the mid-plane separatrix density was increased, the electron temperature at the outer strike point decreased and the ion flux initially increased. At high mid-plane density, the electron temperature was less than a few eV. However, the ion flux did not decrease. Rollover of the ion flux, which is one of important features of the detachment, was not seen in the SONIC simulation with standard parameters.

In order to clarify the key mechanism of the ion flux reduction, the effects of some assumptions regarding the divertor plasma characteristics were investigated. (1) With increasing chemical sputtering yield, the ion flux at the divertor decreased. However, the significant reduction of the ion flux due to the detachment was not seen. (2) By

taking into account the wall pumping effect with the low chemical sputtering yield, rollover of the ion flux appeared. The volume recombination without the large radiation cooling near the X-point seems to be important for rollover. (3) The supersonic flow in the weak detachment phase possibly reduces the ion flux at the target plate. However, in the preliminary check using the SONIC code, the ion flux was not changed although the ion density decreased significantly.

In the case with the wall pumping with the low chemical sputtering yield, rollover of the ion flux was observed. However, the reduction of the ion flux is still small in the high mid-plane density. Further investigation of the reduction mechanism of the ion flux is needed for quantitative modelling of the divertor plasma detachment.

To improve the detachment modelling, the following issues will be investigated in the future.

- The effects of the supersonic flow need to be investigated over a wide parameter range. In addition, the supersonic flow will be self-consistently modeled, as the constant Mach number is artificially given in the present analysis. The radial distribution of the supersonic flow possibly enhances the radial particle diffusion, which decreases the parallel ion flux [7].
- In the experiment, T_e measured at the divertor is often larger than a few eV even in the plasma detached regime, i.e., after rollover of the ion flux. The volume recombination becomes significant at $T_e < 1$ eV. Therefore, if measured T_e is less than 1 eV, the volume recombination is dominant to the detachment. On the other hand, if $T_e >$ a few eV even in the detachment regime, other mechanisms for particle reduction, such as an enhancement of a radial diffusion etc, are needed.
- Generally, in the experiment, the inner divertor is initially detached, and then the outer divertor is detached with increasing core density. In the numerical simulation, this asymmetry is weak. The SOL flow pattern has an important role in the in-out asymmetry of the detachment. The drift effect is one of the important mechanisms to drive the SOL flow. However, the asymmetry is still weak even if the drift effect is taken into account [1]. For the quantitatively modelling of the detachment, other driving mechanism of the SOL flow, such as the orbit-induced flow [10], is needed.

Acknowledgement

This study is partially supported by a Grant-in-Aid for Scientific Research of the Japan Society for the Promotion of Science.

- [1] M. Wischmeier, *et al.*, J. Nucl. Mater. **390-391**, 250 (2009).
- [2] <http://itpa.ipp.mpg.de/>
- [3] H. Kawashima, *et al.*, Plasma Fusion Res. **1**, 031 (2006).
- [4] K. Shimizu, *et al.*, Nucl. Fusion **49**, 065028 (2009).
- [5] A. Loarte, *et al.*, Nucl. Fusion **38**, 331 (1998).
- [6] P. C. Stangeby, Nucl. Fusion **33**, 1695 (1993).
- [7] A. Hatayama, *et al.*, Nucl. Fusion **40**, 2009 (2000).
- [8] T. Takizuka, *et al.*, J. Nucl. Mater. **290-293**, 753 (2001).
- [9] O. Marchuk and M.Z. Tokar, J. Comput. Phys. **227**, 1597-1607 (2007).
- [10] T. Takizuka, *et al.*, to be published in Contrib. Plasma Phys.